Reversible thermal diode and energy harvester with a superconducting quantum interference single-electron transistor

Donald Goury[1] and Rafael Sánchez[2]

[1] *Magistère de Physique Fondamentale, Université Paris-Saclay, F-91405 Orsay, France*
[2] *Departamento de Física Teórica de la Materia Condensada, and Condensed Matter Physics Center (IFIMAC),*
Universidad Autónoma de Madrid, 28049 Madrid, Spain

The density of states of proximitized normal nanowires interrupting superconducting rings can be tuned by the magnetic flux piercing the loop. Using these as the contacts of a single-electron transistor allows to control the energetic mirror asymmetry of the conductor, this way introducing rectification properties. In particular, we show that the system works as a diode that rectifies both charge and heat currents and whose polarity can be reversed by the magnetic field and a gate voltage. We emphasize the role of dissipation at the island. The coupling to substrate phonons enhances the effect and furthermore introduces a channel for phase tunable conversion of heat exchanged with the environment into electrical current.

Nanometric electronic devices demand on-chip components that are driven by temperature gradients or that manage thermal flows. Indeed, nanoscale conductors are interesting in this sense because of their intrinsic nonlinearities, strong spectral features and tunability[1,2]. However, progress in this direction has been slow due to difficulties in the precise experimental detection of heat currents. Only very recently, great advances have been achieved in various mesoscopic configurations[3–8]. They open the way to realize theoretical proposals of heat to current converters[9–17], refrigerators[18–26], thermal transistors[27,28] and diodes[29–32], and valves[33] in the lab.

A thermal rectifier is a system that responds to reversed temperature gradients with currents of different magnitude[34]. For it to work as a thermal diode, forward and backward flows must be of different orders of magnitude. In electronic systems, this is the case for two terminal mesoscopic junctions with strong non-linearities due to Coulomb interactions[29,35–38] or coupled to an additional thermal bath with which it exchanges energy but no charge[39–43]. The performance of the device is then controlled by an external parameter, typically a gate voltage. A requirement is the absence of mirror symmetry, which can also be introduced in the spectral properties of the contacts[30–32,44,45].

At low temperatures, hybrid metallic-superconducting junctions are interesting candidates as one can make use of the properties of single-electron tunneling in strongly interacting islands[46] and of the energy filtering introduced by the gap of the superconducting contacts. Here we investigate a superconducting quantum interference single-electron transistor (SQUISET), sketched in Fig. 1(a). Similar setups have recently been proposed[47] and implemented[48] as single-particle sources and heat valves[49]. It consists on a normal metal island in the strong Coulomb blockade regime such that its occupation fluctuates between $n=0,1$ extra electrons. It can be controlled by the voltage V_g of a plunger gate coupled to it via a capacitance C_g. The island is tunnel-coupled to two short wires that close two respective superconducting rings serving as contacts. Due to the proximity effect,

the wires acquire a minigap[50,51] that is controlled by the magnetic flux, Φ_l, piercing the corresponding ring[47]:

$$\Delta_l = \Delta_0 \left| \cos \frac{\pi \Phi_l}{\Phi_0} \right|, \tag{1}$$

with $l=1,2$ and where Δ_0 is the gap of the superconducting rings and Φ_0 is the flux quantum. This way, the island is effectively coupled to contacts whose spectral properties can be tuned with an external magnetic field. Importantly for our purposes, their asymmetry can also be controlled if the size of the rings is different, as in Fig. 1(b). In particular, one can tune it quite flexibly from configurations with $\Delta_1 \gg \Delta_2$ to the opposite. This introduces the possibility to find a thermal diode whose polarity can be furthermore reverted on chip. The interplay between magnetic and electrostatic control (via Φ
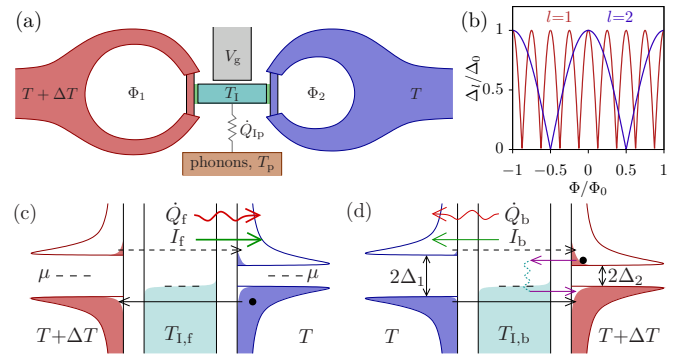

FIG. 1. SQUISET rectifier. (a) A metallic island (controlled by a gate voltage V_g) is tunnel coupled to the weak links of two superconducting loops held at different temperatures, T and $T+\Delta T$, but the same chemical potential μ. (b) The magnetic flux piercing each loop controls the gap of the proximitized contacts, Δ_l, yielding asymmetric spectra when their area is different, such that $\Phi=\Phi_2\neq\Phi_1$ (here, $\Phi_1=4\Phi$). Heat exchanged with a phonon bath at temperature T_p defines the island temperature, T_I. Energy filtering due to the superconducting gaps affect differently the (c) foward and (d) backward currents if $\Delta_1 \neq \Delta_2$.

and V_g, respectively) allows for an enhanced tunability of the device both for heat and thermoelectric currents responding to longitudinal temperature gradients ΔT between terminals 1 and 2. We assume they are at the same chemical potential, $\mu=0$.

Thermalization in the island plays a central role as, on one hand, it establishes a well defined electronic distribution and, on the other hand, it dissipates part of the heat injected from the leads. The forward and backward currents are given by the response of the barrier separating the island, at temperature T_I, and the corresponding cold reservoir, at temperature T. If $\Delta_1 \neq \Delta_2$, the electrons with an energy $\Delta_l < E < \Delta_{l'}$ in the lead l with smaller gap do not contribute to charge transport, but heat the island up, see Fig. 1(d). This has the double effect of (i) introducing an asymmetry between currents that leads to rectification, and of (ii) inducing a different T_I for the forward and backward configurations, as illustrated in Figs. 1(c) and (d). As discussed below, (ii) also has an impact on the rectification.

As heat dissipated at the island is important, the coupling to substrate phonons, at a temperature T_p, cannot be disregarded[52]. It in turn helps to increase the rectification. Interestingly, it also makes the system work as an energy harvester that converts heat exchanged with the phonon bath into an electric current[53].

The metallic island is described by the simple model[46] $H = E_I(n - n_g)^2$, with a charging energy $E_I = e^2/(2C)$ given by its capacitance, C, and the elementary charge e. The charge of the island can be externally tuned via $n_g = C_g V_g/e$. Sequential tunneling events through terminal l into the island are described by the rates:

$$\Gamma_l^+ = \frac{1}{e^2 R_l} \int dE \mathcal{N}_l(E) f_l(E)[1 - f_I(E-U)] \qquad (2)$$

with the associated resistances R_l[54], and the Fermi functions $f_i(E) = \left(1 + e^{E/k_B T_i}\right)^{-1}$. The difference of chemical potentials for this transition is $U = E_I(1 - 2n_g)$. This defines the charge degeneracy point at $n_g = 1/2$. Tunneling out rates, Γ_l^-, are obtained by replacing $f_i(E) \to 1 - f_i(E)$ in Eq. (2). At finite temperatures, subgap states appear in the superconducting leads, which are taken into account by the Dynes density of states:[55]

$$\mathcal{N}_l(E) = \left| \text{Re}\left(\frac{E + i\gamma}{\sqrt{(E + i\gamma)^2 - \Delta_l^2}} \right) \right|, \qquad (3)$$

where γ is the quasiparticle lifetime broadening.

With the particle tunneling rates $\Gamma_l^\pm$ one obtains the steady state occupation of the island p_n via the stationary solution of the rate equations:

$$\dot{p}_0 = -\dot{p}_1 = \sum_l \left(\Gamma_l^- p_1 - \Gamma_l^+ p_0 \right), \qquad (4)$$

with $p_0 + p_1 = 1$. The charge and heat currents into l are hence respectively given by:

$$I_l = -e \left[\Gamma_l^- p_1 - \Gamma_l^+ p_0 \right] \qquad (5)$$

$$\dot{Q}_l = \tilde{\Gamma}_l^- p_1 - \tilde{\Gamma}_l^+ p_0, \qquad (6)$$
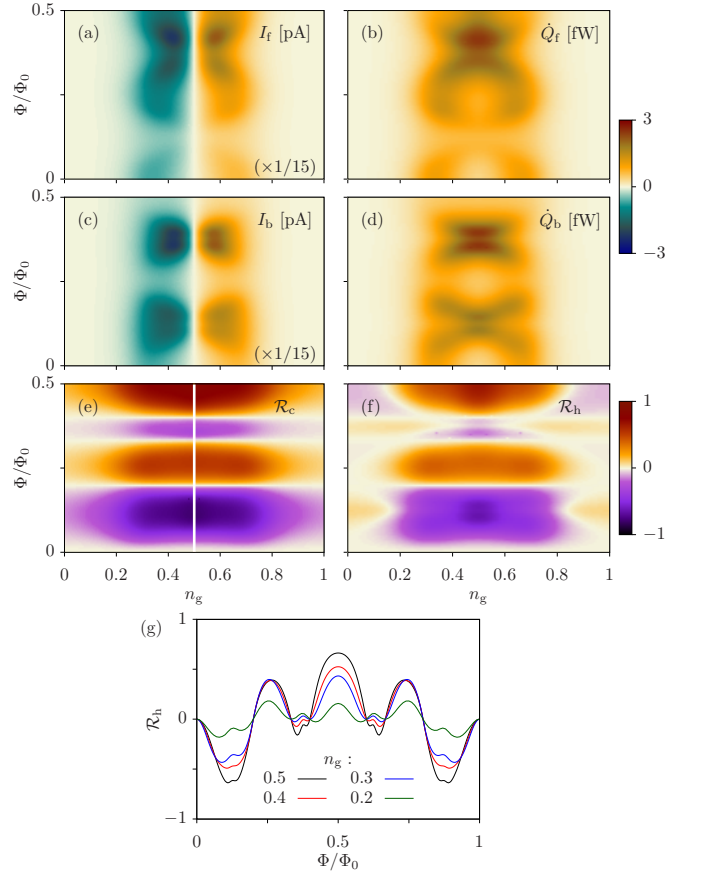

FIG. 2. Forward (a,b) and backward (c,d) charge and heat currents as functions of the gating, n_g, and the magnetic field, $\Phi = \Phi_2 = \Phi_1/4$. The typical sign change of thermoelectric currents and double peak structure of heat currents around $n_g = 1/2$ of single-electron transistors is modulated by the magnetic field. (e,f) Rectification coefficients for the corresponding currents. They change sign when $\Delta_1 = \Delta_2$. (g) Cuts of $\mathcal{R}_h$ in (f) for different n_g show its change of polarity with gating and flux. Parameters: $E_I = 0.25$ meV, $R_1 = R_2 = R_0 = 100$ kΩ, $T = 116$ mK, $\Delta T = 2T$, $T_p = 58$ mK, $\lambda = \lambda_0 = 0.45$ meV²K⁻⁵, and $\gamma = 10^{-3}$ meV.

where $\tilde{\Gamma}_l^\pm$ are obtained by inserting E in the integral of the corresponding $\Gamma_l^\pm$. As no Joule heating is generated in the system, energy conservation is maintained by the heat absorbed at the island: $\dot{Q}_I = -\dot{Q}_1 - \dot{Q}_2$. The temperature of the island is then given by the balance of the heat injected from the leads and the heat exchange with the phononic environment via the equation:

$$\dot{Q}_I(T_I) = \lambda(T_p^5 - T_I^5), \qquad (7)$$

where λ depends on the dimensions of the island and its material[2]. At the superconducting contacts, this exchange is suppressed by the gap[56].

The diode performance is characterized by a difference of the currents under opposite thermal bias. We thus write the forward, $I_f = I_2(T_1 = T + \Delta T, T_2 = T)$, and backward, $I_b = I_1(T_1 = T, T_2 = T + \Delta T)$, charge currents, and
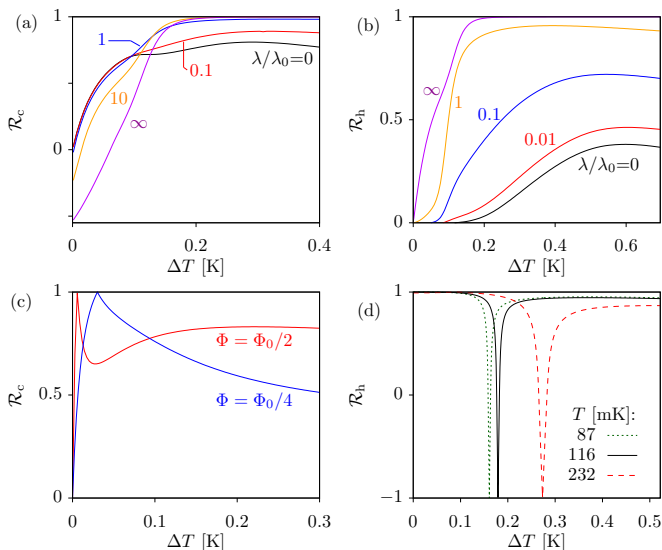
FIG. 3. Effect of the phonon bath. (a,b) Effect of the coupling to the phonon bath, λ, on the charge and heat rectification coefficients, with $T=T_\mathrm{p}$=58 mK. T_I is given by the balance Eq. (7). (c) Charge and (d) heat rectification coefficients for fixed phonon temperature T_p=58 mK. In (c) n_g is chosen such that I_f is maximized for different magnetic fields: $\Phi=\Phi_0/2$ (with n_g=0.49), and $\Phi=\Phi_0/4$ (with n_g=0.3349). In all cases, except when mentioned, parameters are as in Fig. 2, with magnetic fields are fixed such that Δ_1=0.193 meV and Δ_2=0.01 meV, n_g=0.49 and γ=10^{-5} meV.

accordingly for the heat currents $\dot{Q}_\mathrm{f}$ and $\dot{Q}_\mathrm{b}$. With these, we define the rectification coefficients:

$$\mathcal{R}_\mathrm{c} = \frac{|I_\mathrm{f}| - |I_\mathrm{b}|}{\max(|I_\mathrm{f}|,|I_\mathrm{b}|)} \text{ and } \mathcal{R}_\mathrm{h} = \frac{|\dot{Q}_\mathrm{f}| - |\dot{Q}_\mathrm{b}|}{\max(|\dot{Q}_\mathrm{f}|,|\dot{Q}_\mathrm{b}|)}. \quad (8)$$

Note that the sign of $\mathcal{R}_\alpha$ informs of the polarity of the diode, but this is not necessarilly related to the sign of the currents. In particular, for the charge currents, both forward and backward flows change sign around the electron-hole symmetric configurations with $n_\mathrm{g} = 1/2$, as expected for thermoelectric currents in Coulomb blockade systems[57–60], see Fig. 2. However their amplitude depends on the gap of the contacts, and hence $\mathcal{R}_\mathrm{c}$ oscillates and changes sign with the magnetic flux, vanishing when $\Delta_1 = \Delta_2$, see Figs. 2(a), (c) and (e). On the other hand, if the phonons do not introduce an additional thermal gradient, $\dot{Q}_\mathrm{f}$ and $\dot{Q}_\mathrm{b}$ are always positive, see Figs. 2(b) and (d). Note that due to heat flowing into the island, $\mathcal{R}_\mathrm{h}$ also changes its polarity with n_g, as shown in Figs. 2(f) and (g). This is not the case for $\mathcal{R}_\mathrm{c}$ due to charge conservation in the leads ($I_1 + I_2 = 0$).

The maximal rectification coefficients are found close to the electron-hole symmetric configurations. However, additional maxima appear by tuning n_g as an effect of the border of the superconducting gap. Note that $\mathcal{R}_\mathrm{c}$ is not well defined at n_g=1/2, as no thermoelectric currents can be generated in electron-hole symmetric configurations.

We now investigate the crucial effect of the phonon

bath. Let us consider first the case with $T_\mathrm{p} = T$, see Figs. 3(a) and (b). If the coupling to the phonons is strong, the island dissipates the incoming heat from the leads into the environment, so its temperature T_I is not affected (as if it was connected to a thermostat). Then for low ΔT, the gap suppresses the forward current (in this configuration with $\Delta_1 > \Delta_2$), giving $\mathcal{R}_\mathrm{c} < 0$. Increasing the gradient, states over the gap are populated such that I_f and I_b cross, and $\mathcal{R}_\mathrm{c}$ changes sign. The rectification effects are then enhanced and high coefficients $\mathcal{R}_\mathrm{c}$ and $\mathcal{R}_\mathrm{h}$ are achieved, see Figs. 3(a) and (b). With smaller λ, the temperature of the island increases, which is detrimental for the diode performance and avoids the change of sign of $\mathcal{R}_\mathrm{c}$. The optimal values of $\mathcal{R}_\alpha$ are no affected by quasiparticle lifetimes in the experimentally relevant range considered here (with $\gamma \sim 10^{-4}$–10^{-5} meV).

In real configurations, electrons and phonons are not necessarily at the same temperature. The presence of an additional temperature gradient $T_\mathrm{p}-T$ introduces unexpected effects in the rectification properties of the system, due the local breaking of detailed balance. This introduces crossed thermoelectric effects: the phonon bath behaves as a third terminal with which the electronic system exchanges heat (and of course, no charge). This heat exchange can be converted into a contribution of the charge current whose sign is defined by both mirror and electron-hole asymmetries[61,62], even if $\Delta T = 0$. This additional current can flow in the opposite direction as the backward current and eventually cancel it. At that point, only the forward current is finite and we get $\mathcal{R}_\mathrm{c} = 1$, as shown in Fig. 3(c) for two different configurations of the magnetic flux and the gate voltage.

The behaviour of the heat currents is different, see Fig. 3(d). At low temperature gradients ΔT, heat injected from the phonon bath dominates and reverts the forward current, while the backward one is strongly suppressed (due to the gap Δ_1). This leads to $\mathcal{R}_\mathrm{h}\approx 1$. As ΔT increases, the longitudinal heat current dominates, so the forward flow changes sign. At that point, as only the forward current flows, $\mathcal{R}_\mathrm{h}\approx -1$. The position of this sharp feature changes with the temperature of the electrons.

Let us finally further explore the charge current generated by the temperature difference with the phonon bath. For this, we consider the case $T_1 = T_2 = T$ such that there is no longitudinal thermoelectric effect. The conductor is in equilibrium, except for being coupled to phonons at the island. The electrons in the island thermalize at a temperature given by Eq. (7). Thus a local temperature difference is established in the electronic system: In the likely case that $T_\mathrm{p} < T$, the island hence becomes a cold spot, with $T_\mathrm{I} < T$. The effect of having broken electron-hole symmetry (for $n_\mathrm{g} \neq 1/2$) and broken mirror symmetry (due to the superconducting gaps) breaks local detailed balance at both barriers, i.e. $\Gamma_l^+ p_0 \neq \Gamma_l^- p_1$[62]. According to Eq. (5), a net charge current is generated, as sketched in Fig. 4(a) and shown if Fig. 4(b). In this sense, it is a single-electron analogue of a thermocouple in which the electron-hole asymmetry is
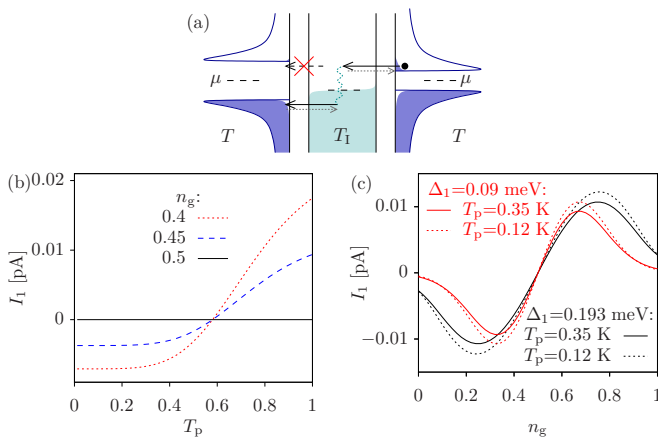
FIG. 4. Conversion of heat exchanged with the phonons. (a) At subgap energies, tunneling is avoided in one terminal (here, the left one due to its larger gap) but not in the right one. The sketched transition hence contributes to transport from terminal 2 to 1 mediated by thermalization at the island. The reversed sequence (marked by dotted grey arrows) is suppressed by broken local detailed balance if $T \neq T_I$ and $n_g \neq 1/2$, leading to a finite current, I_1. (b) It increases with the temperature difference $T - T_p$ and can be tuned with the gate voltage (again for fixed $\Delta_1 = 0.193$ meV, $\Delta_2 = 0.01$ meV). (c) The gating parameter controls the electron-hole asymmetry and hence the sign of the current. The position of the maximum current increases with the gap Δ_1 (here fixing $\Delta_2 = 0.01$ meV). In these plots, $T = 58$ mK and $R_0 = 10$ kΩ.

externally tunable by means of the magnetic field. Contrary to usual thermoelectric heat engines, where heat from a hot bath is transformed into power, the generated charge current is here due to heat emitted into a colder environment. Furthermore, the sign of the current can in this case be controlled either by tuning the gate voltage or the magnetic flux, see Fig. 4(c). As a function of n_g, the current has a maximum when the chemical potential of the island is close to the gap, such that the asymmetry is larger. For higher chemical potentials the effect of the superconductor is reduced and the current is suppressed.

We emphasize that this way, the system has a dual performance as a diode and as a three-terminal converter of environmental heat[53]. Differently from all-normal devices[61,63,64], the presence of the superconductors, apart from introducing the required asymmetric energy filtering, ensures that heat is exchanged with the phonon bath at the mesoscopic region (the island, in our case) only: in the leads, it is strongly suppressed by the gap. This is expected to increase the efficiency. As the temperature difference with the phonons is in principle small, and so are the tunneling couplings, we do not expect the system to be a powerful heat converter. However, this effect can be used as a probe of the environmental temperature.

To conclude, we have investigated the response of a superconducting quantum interference single-electron transistor to temperature gradients. The interplay of Coulomb interactions in the island and phase coherence

in the superconducting rings leads to the rectification of both charge and heat currents. The system then works as a phase and gate tunable thermal diode whose polarity can furthermore be reversed in various configurations. We find that electron-phonon coupling at the metallic island plays an essential role, with heat exchanged with the phonon bath enhancing the diode performance, which is comparable to existing experiments on related configurations[32]. Transport is sensitive to temperature differences with the phonons. This leads to salient features such as the vanishing of forward or backward flows, resulting in optimal diode behaviours with $\mathcal{R}_{c/h} = \pm 1$, or in the generation of charge currents in a conductor which is otherwise in equilibrium (with $T_1 = T_2$). The device is then proposed as a versatile and efficient element for heat management in the nanoscale.

[1] G. Benenti, G. Casati, K. Saito, and R. S. Whitney, Phys. Rep. 694, 1 (2017).

[2] F. Giazotto, T. T. Heikkilä, A. Luukanen, A. M. Savin, and J. P. Pekola, Rev. Mod. Phys. 78, 217 (2006).

[3] F. Giazotto and M. J. Martínez-Pérez, Nature 492, 401 (2012).

[4] M. J. Martínez-Pérez, P. Solinas, and F. Giazotto, J. Low Temp. Phys. 175, 813 (2014).

[5] S. Jezouin, F. D. Parmentier, A. Anthore, U. Gennser, A. Cavanna, Y. Jin, and F. Pierre, Science 342, 601 (2013).

[6] C. Riha, P. Miechowski, S. S. Buchholz, O. Chiatti, A. D. Wieck, D. Reuter, and S. F. Fischer, Appl. Phys. Lett. 106, 083102 (2015).

[7] L. Cui, W. Jeong, S. Hur, M. Matt, J. C. Klöckner, F. Pauly, P. Nielaba, J. C. Cuevas, E. Meyhofer, and P. Reddy, Science 355, 1192 (2017).

[8] B. Dutta, J. T. Peltonen, D. S. Antonenko, M. Meschke, M. A. Skvortsov, B. Kubala, J. König, C. B. Winkelmann, H. Courtois, and J. P. Pekola, Phys. Rev. Lett. 119, 077701 (2017).

[9] R. Sánchez and M. Büttiker, Phys. Rev. B 83, 085428 (2011).

[10] H. Thierschmann, R. Sánchez, B. Sothmann, F. Arnold, C. Heyn, W. Hansen, H. Buhmann, and L. W. Molenkamp, Nature Nanotechnology 10, 854 (2015).

[11] B. Sothmann, R. Sánchez, A. N. Jordan, and M. Büttiker, Phys. Rev. B 85, 205301 (2012).

[12] F. Hartmann, P. Pfeffer, S. Höfling, M. Kamp, and L. Worschech, Phys. Rev. Lett. 114, 146805 (2015).

[13] B. Roche, P. Roulleau, T. Jullien, Y. Jompol, I. Farrer, D. A. Ritchie, and D. C. Glattli, Nature Communications 6, 6738 (2015).

[14] T. E. Humphrey, R. Newbury, R. P. Taylor, and H. Linke, Phys. Rev. Lett. 89, 116801 (2002).

[15] M. Josefsson, A. Svilans, A. M. Burke, E. A. Hoffmann, S. Fahlvik, C. Thelander, M. Leijnse, and H. Linke, Nat. Nanotechnol. 13, 920 (2018).

[16] A. N. Jordan, B. Sothmann, R. Sánchez, and M. Büttiker, Phys. Rev. B 87, 075312 (2013).

[17] G. Jaliel, R. K. Puddy, R. Sánchez, A. N. Jordan, B. Sothmann, I. Farrer, J. P. Griffiths, D. A. Ritchie, and C. G. Smith, arXiv (2019), 1901.10561.

[18] H. Courtois, F. W. J. Hekking, H. Q. Nguyen, and C. B. Winkelmann, J. Low Temp. Phys. 175, 799 (2014).

[19] H. L. Edwards, Q. Niu, and A. L. de Lozanne, Appl. Phys. Lett. **63**, 1815 (1993).

[20] J. R. Prance, C. G. Smith, J. P. Griffiths, S. J. Chorley, D. Anderson, G. A. C. Jones, I. Farrer, and D. A. Ritchie, Phys. Rev. Lett. **102**, 146602 (2009).

[21] M. Nahum, T. M. Eiles, and J. M. Martinis, Appl. Phys. Lett. **65**, 3123 (1994).

[22] M. M. Leivo, J. P. Pekola, and D. V. Averin, Appl. Phys. Lett. **68**, 1996 (1996).

[23] O.-P. Saira, M. Meschke, F. Giazotto, A. M. Savin, M. Möttönen, and J. P. Pekola, Phys. Rev. Lett. **99**, 027203 (2007).

[24] J. P. Pekola, J. V. Koski, and D. V. Averin, Phys. Rev. B **89**, 081309 (2014).

[25] A. V. Feshchenko, J. V. Koski, and J. P. Pekola, Phys. Rev. B **90**, 201407 (2014).

[26] J. V. Koski, A. Kutvonen, I. M. Khaymovich, T. Ala-Nissila, and J. P. Pekola, Phys. Rev. Lett. **115**, 260602 (2015).

[27] H. Thierschmann, F. Arnold, M. Mittermüller, L. Maier, C. Heyn, W. Hansen, H. Buhmann, and L. W. Molenkamp, New J. Phys. **17**, 113003 (2015).

[28] R. Sánchez, H. Thierschmann, and L. W. Molenkamp, Phys. Rev. B **95**, 241401 (2017).

[29] R. Scheibner, M. König, D. Reuter, A. D. Wieck, C. Gould, H. Buhmann, and L. W. Molenkamp, New J. Phys. **10**, 083016 (2008).

[30] F. Giazotto and F. S. Bergeret, Appl. Phys. Lett. **103**, 242602 (2013).

[31] M. J. Martínez-Pérez and F. Giazotto, Appl. Phys. Lett. **102**, 182602 (2013).

[32] M. J. Martínez-Pérez, A. Fornieri, and F. Giazotto, Nat. Nanotechnol. **10**, 303 (2015).

[33] A. Ronzani, B. Karimi, J. Senior, Y.-C. Chang, J. T. Peltonen, C. Chen, and J. P. Pekola, Nat. Phys. **14**, 991 (2018).

[34] G. Benenti, G. Casati, C. Mejía-Monasterio, and M. Peyrard, "From thermal rectifiers to thermoelectric devices," in *Thermal Transport in Low Dimensions: From Statistical Physics to Nanoscale Heat Transfer*, edited by S. Lepri (Springer International Publishing, Cham, 2016) pp. 365–407.

[35] T. Ruokola, T. Ojanen, and A.-P. Jauho, Phys. Rev. B **79**, 144306 (2009).

[36] M. A. Sierra and D. Sánchez, Mater. Today:. Proc. **2**, 483 (2015).

[37] L. Vannucci, F. Ronetti, G. Dolcetto, M. Carrega, and M. Sassetti, Phys. Rev. B **92**, 075446 (2015).

[38] A. Marcos-Vicioso, C. López-Jurado, M. Ruiz-Garcia, and R. Sánchez, Phys. Rev. B **98**, 035414 (2018).

[39] A. Fornieri, M. J. Martínez-Pérez, and F. Giazotto, Appl. Phys. Lett. **104**, 183108 (2014).

[40] R. Sánchez, B. Sothmann, and A. N. Jordan, New J. Phys. **17**, 075006 (2015).

[41] J.-H. Jiang, M. Kulkarni, D. Segal, and Y. Imry, Phys. Rev. B **92**, 045309 (2015).

[42] G. Rosselló, R. López, and R. Sánchez, Phys. Rev. B **95**, 235404 (2017).

[43] R. Sánchez, H. Thierschmann, and L. W. Molenkamp, New J. Phys. **19**, 113040 (2017).

[44] D. Oettinger, R. Chitra, and J. Restrepo, Eur. Phys. J. B **87**, 224 (2014).

[45] L. Bours, B. Sothmann, M. Carrega, E. Strambini, A. Braggio, E. M. Hankiewicz, L. W. Molenkamp, and F. Giazotto, Phys. Rev. Appl. **11**, 044073 (2019).

[46] D. V. Averin and K. K. Likharev, J. Low Temp. Phys. **62**, 345 (1986).

[47] E. Enrico and F. Giazotto, Phys. Rev. Appl. **5**, 064020 (2016).

[48] E. Enrico, E. Strambini, and F. Giazotto, Sci. Rep. **7**, 13492 (2017).

[49] E. Strambini, F. S. Bergeret, and F. Giazotto, Appl. Phys. Lett. **105**, 082601 (2014).

[50] T. T. Heikkilä, J. Särkkä, and F. K. Wilhelm, Phys. Rev. B **66**, 184513 (2002).

[51] H. Le Sueur, P. Joyez, H. Pothier, C. Urbina, and D. Esteve, Phys. Rev. Lett. **100**, 197002 (2008).

[52] F. C. Wellstood, C. Urbina, and J. Clarke, Phys. Rev. B **49**, 5942 (1994).

[53] B. Sothmann, R. Sánchez, and A. N. Jordan, Nanotechnology **26**, 032001 (2015).

[54] For typical experimental resistances of 10–100 kΩ, the tunneling rates set an upper bound on the device frequency of around 10–100 GHz.

[55] J. P. Pekola, V. F. Maisi, S. Kafanov, N. Chekurov, A. Kemppinen, Y. A. Pashkin, O.-P. Saira, M. Möttönen, and J. S. Tsai, Phys. Rev. Lett. **105**, 026803 (2010).

[56] A. V. Timofeev, C. P. García, N. B. Kopnin, A. M. Savin, M. Meschke, F. Giazotto, and J. P. Pekola, Phys. Rev. Lett. **102**, 017003 (2009).

[57] A. A. M. Staring, L. W. Molenkamp, B. W. Alphenaar, H. van Houten, O. J. A. Buyk, M. A. A. Mabesoone, C. W. J. Beenakker, and C. T. Foxon, Europhysics Letters (EPL) **22**, 57 (1993).

[58] A. S. Dzurak, C. G. Smith, M. Pepper, D. A. Ritchie, J. E. F. Frost, G. A. C. Jones, and D. G. Hasko, Solid State Commun. **87**, 1145 (1993).

[59] C. W. J. Beenakker and A. A. M. Staring, Phys. Rev. B **46**, 9667 (1992).

[60] P. A. Erdman, F. Mazza, R. Bosisio, G. Benenti, R. Fazio, and F. Taddei, Phys. Rev. B **95**, 245432 (2017).

[61] O. Entin-Wohlman, Y. Imry, and A. Aharony, Phys. Rev. B **82**, 115314 (2010).

[62] R. Sánchez, "Transport out of locally broken detailed balance," in *Coupled Mathematical Models for Physical and Biological Nanoscale Systems and Their Applications*, edited by L. L. Bonilla, E. Kaxiras, and R. Melnik (Springer International Publishing, Cham, 2018) pp. 51–64.

[63] R. Bosisio, G. Fleury, J.-L. Pichard, and C. Gorini, Phys. Rev. B **93**, 165404 (2016).

[64] J.-H. Jiang, O. Entin-Wohlman, and Y. Imry, Phys. Rev. B **85**, 075412 (2012).